Bounding Imprecise Failure Probabilities in Structural Mechanics based on Maximum Standard Deviation

Marc Fina[a,*], Celine Lauff[a], Matthias G. R. Faes[b], Marcos A. Valdebenito[c], Werner Wagner[a], Steffen Freitag[a]

[a]*Karlsruhe Institute of Technology, Institute for Structural Analysis, Kaiserstr. 12, 76131 Karlsruhe, Germany*
[b]*TU Dortmund University, Chair for Reliability Engineering, Leonhard-Euler Strasse 5, 44227, Dortmund, Germany*
[c]*Faculty of Engineering and Sciences, Universidad Adolfo Ibáñez, Av. Padre Hurtado 750, 2562340 Viña del Mar, Chile*

Abstract

This paper proposes a framework to calculate the bounds on failure probability of linear structural systems whose performance is affected by both random variables and interval variables. This kind of problems is known to be very challenging, as it demands coping with aleatoric and epistemic uncertainty explicitly. Inspired by the framework of the operator norm theorem, it is proposed to consider the maximum standard deviation of the structural response as a proxy for detecting the crisp values of the interval parameters, which yield the bounds of the failure probability. The scope of application of the proposed approach comprises linear structural systems, whose properties may be affected by both aleatoric and epistemic uncertainty and that are subjected to (possibly imprecise) Gaussian loading. Numerical examples indicate that the application of such proxy leads to substantial numerical advantages when compared to a traditional double-loop approach for coping with imprecise failure probabilities. In fact, the proposed framework allows to decouple the propagation of aleatoric and epistemic uncertainty.

Keywords: Linear structures, Gaussian loading, Standard deviation, Failure probability, Aleatoric uncertainty, Epistemic uncertainty

---

Highlights:

- Decoupled approach allows to estimate bounds of failure probability.
- Focus on linear structures affected by aleatoric and epistemic uncertainty.
- Loading characterized as Gaussian process, may be affected by imprecision.
- Maximum standard deviation offers suitable proxy for bounding probability.

*Corresponding author
Email address: marc.fina@kit.edu (Marc Fina)

1. Introduction

One of the main trends in engineering design of the last few decades is to evolve from real-life experiments to in-silico structural evaluations. Numerical techniques to evaluate the differential equations that describe the effect of occurring loads on the structure under assessment, from the micro to macro scale, as such have become indispensable. However, the main criticism with respect to such techniques is that the predicted results in these in-silico experiments often diverge from those obtained in their real-life counterparts. The source of this divergence is the fact that both, the structure that is being observed, as well as the process of observing the structure are subjected to uncertainties. In the former case, uncertainty creeps in the problem formulation through variable material properties (e.g., Young's modulus) or loading conditions (e.g., wind loads). These uncertainties are also referred to as *aleatory* uncertainties and are best characterized using probabilistic methods, such as described in [1]. In the latter case, the uncertainty stems from limited observation capabilities. In essence, an analysis of a structure is always constrained, be it by (experimental) costs, time or the resolution of our measurement devices. These *epistemic* uncertainties may be described by probabilistic techniques in certain cases, but generally set-theoretical methods such as intervals [2] are better suited.

As may be understood from the preceding explanation, the joint occurrence of epistemic and aleatoric uncertainties in numerical models, including their corresponding uncertainty models, is more the standard than the exception. As such, to properly address the divergence between real-life and in-silico experiments, both have to be taken into account jointly. In this context, some authors make the distinction between hybrid reliability analysis [3] or polymorphic uncertainty modeling [4] when the aleatoric and epistemic parameters are defined on separate model variables and imprecise probabilistic analysis [5, 6] when both uncertainties affect the same model variables (e.g., a random parameter with interval-valued distribution parameters, e.g., an interval mean value). While the modeling of uncertainties using these tools is very versatile, it also poses a major challenge from a numerical point of view when performing uncertainty quantification, as both sources of uncertainty (aleatoric and epistemic) must be propagated to the response of the structural system. It is important to note that such propagation is conducted under the condition that the effects of aleatoric and epistemic uncertainty are kept separated. This implies that both sources of uncertainty are usually propagated by means of the so-called double loop approaches, where the outer loop takes care of epistemic uncertainty while the inner loop deals with aleatoric uncertainty [7]. Double loop approaches are generally highly accurate, but the corresponding computational cost becomes quickly intractable, especially when industrially sized models are considered. Therefore, a considerable amount of research is focused on finding more efficient techniques for the propagation of uncertainty through numerical simulation models. A multitude of numerical schemes have been proposed to propagate these types of uncertainties. Examples of such approaches are based on Extended Monte Carlo simulation [8], surrogate modeling schemes [9, 10, 11], Bayesian probabilistic propagation [12], [13], Line Sampling [14] or importance sampling [15, 16]. For a complete overview of literature on this topic, the reader is referred to the recent review papers [3] and [6]. A latest development in this context is based on operator norm theory to decouple the double loop into a deterministic optimization, followed by a single reliability analysis per bound on the reliability, as introduced in [17, 18], which is capable of reducing the corresponding computational cost by several orders of magnitude. The method was later extended to more general loading conditions in [19] and to non-linear models in [20]. The current state-of-the-art in operator norm theory is that the approach can deal with hybrid uncertainty and imprecise probability on the loading side (including moderate non-linearity), whereas concerning the model side, only epistemic uncertainty is possible so far. This greatly hinders the application of the operator norm framework in areas, where the model description itself is subject to considerable aleatoric uncertainty, as is the case in e.g., parts produced using advanced manufacturing techniques (e.g., additive manufacturing or composite materials), natural materials such as wood [21], shell buckling with geometrical imperfections [10] or applications in soil engineering [22].

In this paper, we propose a framework to allow the propagation of both aleatoric and epistemic uncertainties at both the model side and the loading. Hereto, we first illustrate the equivalence of the operator norm with the maximum standard deviation of a response under certain conditions. Inspired by this equivalence, we then illustrate how this maximum standard deviation can be approximated efficiently under the most general definition of the governing uncertainties by means of a first-order series expansion without resorting to random sampling. Three engineering examples are presented to show the effectiveness of the approach in this situation.

The paper is structured as follows; Section 2 gives a rigorous formulation of the problem considered in this manuscript. Section 3 explains the proposed approach highlighted above in detail. Section 4 illustrates the method by means of three engineering examples: an FE model of a Reissner-Mindlin plate subjected to imprecise stochastic loading, a model of a single-degree-of-freedom oscillator with random mass and interval-valued stiffness subject to a stochastic ground acceleration, and a three-story concrete frame modeled as a three-mass oscillator that is subjected to an earthquake loading. Finally, Section 5 lists the conclusions of this work.

2. Formulation of the problem

2.1. General Remarks

This contribution proposes a framework to calculate the bounds on failure probability. The focus is on linear structural systems which are subject to static or dynamic loading. It is assumed that the loading can be modeled as an imprecise Gaussian process, as discussed in detail in Section 2.2. Furthermore, the structural properties can be uncertain and modeled by means of random variables and/or interval variables, as considered in Section 2.3. In consequence, the probability of failure of the structural system becomes interval-valued, as analyzed in Sections 2.4 and 2.5.

2.2. Imprecise Gaussian loading

Consider a Gaussian process f whose mean and covariance are μ and γ, respectively. It is assumed that these two quantities are parametrized with respect to a vector $\boldsymbol{\theta}_f$ that represents certain physical properties of the Gaussian process [23]. Hence, $\mu = \mu(\boldsymbol{\theta}_f)$ and $\gamma = \gamma(\boldsymbol{\theta}_f)$. Considering a discrete time or space representation of this process, the associated mean vector is denoted as $\boldsymbol{\mu}(\boldsymbol{\theta}_f)$ while the covariance matrix is denoted as $\boldsymbol{\Gamma}(\boldsymbol{\theta}_f)$. Thus, the Gaussian process is represented in its discrete form by means of the Karhunen-Loève expansion, see [24]:

$$\boldsymbol{f}(\boldsymbol{\theta}_f, \boldsymbol{z}) = \boldsymbol{\mu}(\boldsymbol{\theta}_f) + \boldsymbol{B}(\boldsymbol{\theta}_f)\,\boldsymbol{z}, \tag{1}$$

where $\boldsymbol{f}$ is a realization of the Gaussian loading, which is a $n_f \times 1$ vector; n_f denotes the number of time or space discretization points; $\boldsymbol{\mu}$ is a $n_f \times 1$ vector representing the mean of the Gaussian process; $\boldsymbol{z}$ is a realization of a standard Gaussian random variable vector $\boldsymbol{Z}$ of dimension $n_z \times 1$ and whose probability density function is denoted as $p_{\boldsymbol{Z}}(\boldsymbol{z})$; and $\boldsymbol{B}$ is a matrix defined as:

$$\boldsymbol{B}(\boldsymbol{\theta}_f) = \boldsymbol{\Psi}(\boldsymbol{\theta}_f)\left(\boldsymbol{\Lambda}(\boldsymbol{\theta}_f)\right)^{1/2}, \tag{2}$$

where $\boldsymbol{\Psi}$ is a matrix of dimension $n_f \times n_z$ containing the first n_z eigenvectors of the covariance matrix $\boldsymbol{\Gamma}$; $\boldsymbol{\Lambda}$ is a matrix whose diagonal contains the first n_z eigenvalues of the covariance matrix

$\mathbf{\Gamma}$, such that $\mathbf{\Gamma} \approx \mathbf{\Psi}\mathbf{\Lambda}\mathbf{\Psi}^T$ (where $(\cdot)^T$ denotes transpose of the argument); and n_z is the number of terms retained for the Karhunen-Loève expansion ($n_z \leq n_f$, see, e.g. [1]).

As noted from Eqs. (1, 2), the Gaussian process depends on vector $\boldsymbol{\theta}_f$. In turn, this vector contains relevant information regarding the physical properties of the process, such as dominant frequencies or spectral intensity, to name a few. In practical situations, it may occur that identifying precise values for $\boldsymbol{\theta}_f$ may be challenging due to issues such as lack of knowledge. In such case, it may be appropriate to characterize the associated epistemic uncertainty in terms of intervals, such that $\boldsymbol{\theta}_f \in \left[\underline{\boldsymbol{\theta}}_f, \overline{\boldsymbol{\theta}}_f\right]$, where $\underline{(\cdot)}$ and $\overline{(\cdot)}$ denote the lower and upper bounds of a vector. Under such assumption, Eq. (1) allows characterizing the uncertainty in the loading as an imprecise Gaussian process, as it is affected by epistemic uncertainty (associated with $\boldsymbol{\theta}_f$) as well as by aleatoric uncertainty (associated with $\boldsymbol{z}$).

2.3. Structural model and its response

It is considered that the structural model under analysis possesses a total of n_r responses of interest, which are collected in vector $\boldsymbol{\eta}^*$. In view of the assumption of linearity of the structural response [25], this response vector can be expressed as (see Appendix A):

$$\boldsymbol{\eta}^*(\boldsymbol{\theta}_s, \boldsymbol{\theta}_f, \boldsymbol{y}, \boldsymbol{z}) = \boldsymbol{A}(\boldsymbol{\theta}_s, \boldsymbol{y})\boldsymbol{f}(\boldsymbol{\theta}_f, \boldsymbol{z}), \tag{3}$$

where $\boldsymbol{A}$ is a matrix of dimension $n_r \times n_f$ associated with the structural response; $\boldsymbol{\theta}_s$ and $\boldsymbol{y}$ denote two vectors of parameters that affect structural performance and that are uncertain. Vector $\boldsymbol{\theta}_s$ groups parameters regarded as epistemic, whose uncertainty is characterized by means of intervals, that is $\boldsymbol{\theta}_s \in \left[\underline{\boldsymbol{\theta}}_s, \overline{\boldsymbol{\theta}}_s\right]$. Vector $\boldsymbol{y}$ groups parameters of the aleatoric type whose uncertainty is characterized by means of a random variable vector $\boldsymbol{Y}$ with probability density $p_{\boldsymbol{Y}}(\boldsymbol{y})$. It is assumed that random variables grouped in vector $\boldsymbol{Y}$ are independent among them as well as with respect to $\boldsymbol{Z}$.

For practical design purposes, it is of interest monitoring that none of the structural responses (in absolute value) exceed prescribed thresholds [26]. These thresholds are collected in vector $\boldsymbol{b}$ of dimension n_r. Assuming that all components of the threshold vector $\boldsymbol{b}$ are different from zero (that is, $\boldsymbol{b} = [b_1, \ldots, b_{n_r}]^T \neq [0, \ldots, 0]^T$) and recalling the load representation as cast in Eq. (1), it is possible to define a so-called normalized response vector $\boldsymbol{\eta}$, that is:

$$\boldsymbol{\eta}(\boldsymbol{\theta}, \boldsymbol{y}, \boldsymbol{z}) = \overline{\boldsymbol{c}}(\boldsymbol{\theta}, \boldsymbol{y}) + \boldsymbol{C}(\boldsymbol{\theta}, \boldsymbol{y})\boldsymbol{z}, \tag{4}$$

where $\boldsymbol{\theta}$ is a vector that collects epistemic parameters affecting structural behavior and loading, that is $\boldsymbol{\theta} = \left[\boldsymbol{\theta}_s^T, \boldsymbol{\theta}_f^T\right]^T$; $\overline{\boldsymbol{c}}$ is a vector of dimension n_r defined as:

$$\overline{\boldsymbol{c}}(\boldsymbol{\theta}, \boldsymbol{y}) = \begin{bmatrix} b_1 & & \\ & \ddots & \\ & & b_{n_r} \end{bmatrix}^{-1} \boldsymbol{A}(\boldsymbol{\theta}_s, \boldsymbol{y})\boldsymbol{\mu}(\boldsymbol{\theta}_f), \tag{5}$$

and $\boldsymbol{C}$ is a $n_r \times n_z$ matrix defined as:

$$\boldsymbol{C}(\boldsymbol{\theta}, \boldsymbol{y}) = \begin{bmatrix} b_1 & & \\ & \ddots & \\ & & b_{n_r} \end{bmatrix}^{-1} \boldsymbol{A}(\boldsymbol{\theta}_s, \boldsymbol{y})\boldsymbol{B}(\boldsymbol{\theta}_f). \tag{6}$$

Eq. (4) provides a compact and convenient means for expressing structural response in a normalized fashion. Indeed, as the threshold vector is included in its formulation, it is straightforward to note that $\boldsymbol{\eta}$ is actually a dimensionless vector. Furthermore, whenever the absolute value of any of the components of $\boldsymbol{\eta}$ exceeds 1, it becomes evident that a design criterion is no longer fulfilled [26].

2.4. Failure probability

The chance that an undesirable behavior occurs (that is, any of the responses contained in $\boldsymbol{\eta}$ exceeding 1 in absolute value) is calculated by means of the following classical integral [23]:

$$p_F(\boldsymbol{\theta}) = \int_{\boldsymbol{z} \in \mathbb{R}^{n_z}} \int_{\boldsymbol{y} \in \Omega_y} I_F(\boldsymbol{\theta}, \boldsymbol{y}, \boldsymbol{z}) p_{\boldsymbol{Y}}(\boldsymbol{y}) p_{\boldsymbol{Z}}(\boldsymbol{z}) d\boldsymbol{y} d\boldsymbol{z}, \tag{7}$$

where p_F denotes the failure probability; and $I_F(\cdot, \cdot, \cdot)$ is the indicator function, which is equal to one in case $\|\bar{\boldsymbol{c}}(\boldsymbol{\theta}, \boldsymbol{y}) + \boldsymbol{C}(\boldsymbol{\theta}, \boldsymbol{y})\boldsymbol{z}\|_\infty \geq 1$ and zero, otherwise; note that $\|\cdot\|_\infty$ denotes the infinity pseudo-norm.

2.5. Interval failure probability

Note that the failure probability as cast in Eq. (7) synthesizes the level of safety of a structure with respect to aleatoric uncertainty conditional on $\boldsymbol{\theta}$. In turn, $\boldsymbol{\theta}$ collects uncertain parameters of the epistemic type, which are characterized as interval valued, that is $\boldsymbol{\theta} \in \left[\underline{\boldsymbol{\theta}}, \overline{\boldsymbol{\theta}}\right]$. Hence, it is evident that the failure probability p_F becomes interval valued as well [22]. Naturally, it is of interest determining the lower and upper bounds of this probability (denoted as $\underline{p}_F$ and $\overline{p}_F$, respectively), that is:

$$\underline{p}_F = \min_{\boldsymbol{\theta} \in [\underline{\boldsymbol{\theta}}, \overline{\boldsymbol{\theta}}]} \left(p_F(\boldsymbol{\theta})\right) \tag{8}$$

$$\overline{p}_F = \max_{\boldsymbol{\theta} \in [\underline{\boldsymbol{\theta}}, \overline{\boldsymbol{\theta}}]} \left(p_F(\boldsymbol{\theta})\right), \tag{9}$$

where $\min(\cdot)$ and $\max(\cdot)$ denote the minimum and maximum value, respectively, of the argument. In essence, Eqs. (8, 9) constitute so-called *double loop* problems: in the outer loop, one must perform optimization in order to locate the minimum/maximum of the failure probability with respect to the epistemic parameters $\boldsymbol{\theta}$; while in the inner loop, one must propagate aleatoric uncertainty in order to estimate the failure probability for a given value of $\boldsymbol{\theta}$ (see Eq. (7)). Thus, the solution of these two optimization problems can be extremely costly from a numerical point of view. Therefore, in the following, an approach that can alleviate such numerical burden is proposed.

3. Standard Deviation as a Proxy of the Failure Probability

3.1. Operator Norm Theorem: Brief Overview

This subsection briefly retakes the theory behind the operator norm as considered in [17, 18, 27, 28]. Let $\boldsymbol{D} : \mathbb{R}^{d_v} \mapsto \mathbb{R}^{d_r}$ be a continuous linear map between two normed vector spaces $\mathbb{R}^{d_v}$ and $\mathbb{R}^{d_r}$ and $\|\bullet\|_{p^i}$ be a particular $\mathcal{L}_{p^i}$ norm on these vector spaces with $p^i \in [1, \infty)$. It is assumed that this map depends on a vector $\boldsymbol{\zeta}$, that is, $\boldsymbol{D}(\boldsymbol{\zeta})$. Then, there is a number $c \in \mathbb{R}$ such that:

$$\|\boldsymbol{D}(\boldsymbol{\zeta})\boldsymbol{v}\|_{p^1} \leq |c(\boldsymbol{\zeta})| \cdot \|\boldsymbol{v}\|_{p^2}, \tag{10}$$

for all $\boldsymbol{v} \in \mathbb{R}^{d_v}$, where $\|\boldsymbol{v}\|_{p^i}$ is constructed according to $\|\boldsymbol{v}\|_{p^i} = \left(\sum_{j=1}^{d_v} |v_j|^{p^i}\right)^{1/p^i}$, with $v_j \in \boldsymbol{v}$. Note that for the case of $p^i = \infty$, one retrieves the well-known infinity norm of a vector, that is

$\|\boldsymbol{v}\|_{p^i=\infty} = \max_{j=1,\ldots,d_v} (|v_j|)$. Equivalently, Eq. (10) can be rewritten as:

$$\|\boldsymbol{\xi}(\boldsymbol{\zeta})\|_{p^1} \leq |c(\boldsymbol{\zeta})|\|\boldsymbol{v}\|_{p^2}, \tag{11}$$

where $\boldsymbol{\xi}(\boldsymbol{\zeta}) = \boldsymbol{D}(\boldsymbol{\zeta})\boldsymbol{v}$. A measure for *how much* $\boldsymbol{D}(\boldsymbol{\zeta})$ increases the length of the vector $\boldsymbol{v}$ in the maximum case, is given by the operator norm $\|\boldsymbol{D}(\boldsymbol{\zeta})\|_{p^1,p^2}$ [29], which is defined as:

$$||\boldsymbol{D}(\boldsymbol{\zeta})||_{p^1,p^2} = \inf\left\{c \geq 0 : \|\boldsymbol{D}(\boldsymbol{\zeta})\boldsymbol{v}\|_{p^1} \leq |c(\boldsymbol{\zeta})| \cdot \|\boldsymbol{v}\|_{p^2} \quad \forall \boldsymbol{v} \in \mathbb{R}^{n_v}\right\}, \tag{12}$$

or equivalently:

$$||\boldsymbol{D}(\boldsymbol{\zeta})||_{p^1,p^2} = \sup\left\{\frac{\|\boldsymbol{D}(\boldsymbol{\zeta})\boldsymbol{v}\|_{p^1}}{\|\boldsymbol{v}\|_{p^2}} : \boldsymbol{v} \in \mathbb{R}^{n_v} \text{ with } \boldsymbol{v} \neq 0\right\}. \tag{13}$$

The calculation of a particular $||\boldsymbol{D}(\boldsymbol{\zeta})||_{p^1,p^2}$ norm clearly depends on the particular choice of p^1 and p^2. For the particular choice of p^1=∞ and $p^2 = 2$ [29] and under the assumption that $\boldsymbol{v}$ is a realization of standard normal random variable vector, it can be shown that $||\boldsymbol{D}(\boldsymbol{\zeta})||_{p^1,p^2}$ effectively corresponds to the maximum standard deviation of $\boldsymbol{\xi}$ (see Appendix B). This salient feature was used in earlier work to bound the first excursion probability of imprecise structures subjected to imprecise stochastic loads [18, 27]. In essence, it is assumed in those contributions that the parameter vector $\boldsymbol{\zeta}$ could represent interval-valued quantities that affect the structural behaviour and/or load representation. Thus, the operator norm is employed as a means for identifying the crisp values of $\boldsymbol{\zeta}$ that would lead to the minimum and maximum values of the operator norm (as cast in Eq. (12) or (13)). In other words, one aims at determining the two sets of values of $\boldsymbol{\zeta}$ that induce less and most strechting that matrix $\boldsymbol{D}(\boldsymbol{\zeta})$ (that represents the system's properties) exerts over the external load (represented by $\boldsymbol{v}$ in this case), respectively. In turn, those two sets of values for $\boldsymbol{\zeta}$ are then employed to perform two reliability analysis, which yield the lower and upper values of the failure probability, respectively. For a more detailed explanation on the operator norm, it is referred to [18, 27].

3.2. Standard Deviation as a Proxy for Determining Bounds of the Failure Probability

As already discussed in Section 2, the focus of this work is on bounding the failure probability associated with a linear structural system affected by epistemic and aleatoric uncertainty which is subjected to imprecise Gaussian loading. Based on the concepts presented in Section 3.1, it is noted that under certain conditions, the application of the operator norm theorem is equivalent to calculating the maximum standard deviation of the response. Inspired by such approach, it is proposed in this work to consider the maximum standard deviation of the response of a system as a proxy for bounding the failure probability. Hence, the set of values of the interval parameters that leads to a minimum/maximum value of the failure probability are identified by solving the following two optimization problems:

$$\underline{\boldsymbol{\theta}}^* = \underset{\boldsymbol{\theta}\in[\underline{\boldsymbol{\theta}},\overline{\boldsymbol{\theta}}]}{\operatorname{argmin}} \left(\sigma_{\max}(\boldsymbol{\theta})\right) \tag{14}$$

$$\overline{\boldsymbol{\theta}}^* = \underset{\boldsymbol{\theta}\in[\underline{\boldsymbol{\theta}},\overline{\boldsymbol{\theta}}]}{\operatorname{argmax}} \left(\sigma_{\max}(\boldsymbol{\theta})\right), \tag{15}$$

where argmin and argmax are functions that return the argument for which a given function is minimized or maximized, respectively; $\underline{\boldsymbol{\theta}}^*$ and $\overline{\boldsymbol{\theta}}^*$ denote the set of values of the uncertain interval parameters which yield the minimum/maximum value of $\sigma_{\max}$; and $\sigma_{\max}$ denotes the maximum standard deviation of the response $\boldsymbol{\eta}$, that is:

$$\sigma_{\max}(\boldsymbol{\theta}) = \max_{j=1,\ldots,n_r} \left(\left(\mathcal{V}\left[\eta_j\right]\right)^{1/2} \right), \tag{16}$$

where $\mathcal{V}[\cdot]$ denotes variance of the argument and η_k is the k-th element of the normalized response vector $\boldsymbol{\eta}$. Taking into account the above formulation, the bounds of the failure probability are given approximately by:

$$\underline{p}_F \approx p_F\left(\underline{\boldsymbol{\theta}}^*\right) \tag{17}$$

$$\overline{p}_F \approx p_F\left(\overline{\boldsymbol{\theta}}^*\right). \tag{18}$$

The solution of the optimization problems in Eqs. (14, 15) is quite advantageous from a numerical point of view: it demands calculating the maximum standard deviation of the normalized response $\sigma_{\max}(\boldsymbol{\theta})$, whose determination is usually much less involved than that of the failure probability. Details about the calculation of $\sigma_{\max}(\boldsymbol{\theta})$ are discussed in the following.

3.3. Determination of the Maximum Standard Deviation of the Response

The calculation of the maximum standard deviation of the response $\sigma_{\max}$ for a specified value of the epistemic parameters $\boldsymbol{\theta}$ could be carried out by means of, e.g., Monte Carlo simulation. Such an approach would demand generating N samples of the vector of uncertain structural parameters and loading, that is $\boldsymbol{y}^{(l)} \sim p_{\boldsymbol{Y}}(\boldsymbol{y}),\ \boldsymbol{z}^{(l)} \sim p_{\boldsymbol{Z}}(\boldsymbol{z}),\ l = 1, \ldots, N$ and evaluating the normalized structural response for each of those samples. Thus, the estimator for the maximum standard deviation based on Monte Carlo simulation (which is denoted as $\sigma^S_{\max}(\boldsymbol{\theta})$) is equal to:

$$\sigma_{\max}(\boldsymbol{\theta}) \approx \sigma^S_{\max}(\boldsymbol{\theta}) = \max_{j=1,\ldots,n_r} \left(\sqrt{\frac{1}{N-1} \sum_{l=1}^{N} \left(\eta_j \left(\boldsymbol{\theta}, \boldsymbol{y}^{(l)}, \boldsymbol{z}^{(l)} \right) - \mu^S_j(\boldsymbol{\theta}) \right)^2 } \right), \tag{19}$$

where $\mu^S_j(\boldsymbol{\theta})$ is the mean value vector of the j-th normalized response, which is calculated as:

$$\mu^S_j(\boldsymbol{\theta}) = \frac{1}{N} \sum_{l=1}^{N} \eta_j \left(\boldsymbol{\theta}, \boldsymbol{y}^{(l)}, \boldsymbol{z}^{(l)} \right). \tag{20}$$

While the application of Monte Carlo simulation for estimating the maximum standard deviation is feasible, it may be undesirable from a numerical point of view for two issues. First, it requires performing simulation, which is numerically demanding. Second, it provides estimates instead of precise quantities; in general, it is challenging to perform optimization with estimates. In view of these challenges, the sought maximum standard deviation is calculated in an approximate, closed-form approach, as described below.

It is assumed that vector $\overline{\boldsymbol{c}}(\boldsymbol{\theta}, \boldsymbol{y})$ and matrix $\boldsymbol{C}(\boldsymbol{\theta}, \boldsymbol{y})$ as defined in Eqs. (5, 6), respectively, can be represented approximately as:

$$\overline{\boldsymbol{c}}(\boldsymbol{\theta}, \boldsymbol{y}) \approx \overline{\boldsymbol{c}}_0(\boldsymbol{\theta}, \boldsymbol{y}^0) + \sum_{i=1}^{n_y} \overline{\boldsymbol{c}}_i(\boldsymbol{\theta}, \boldsymbol{y}^0)(y_i - y^0_i) \tag{21}$$

$$\boldsymbol{C}(\boldsymbol{\theta}, \boldsymbol{y}) \approx \boldsymbol{C}_0(\boldsymbol{\theta}, \boldsymbol{y}^0) + \sum_{i=1}^{n_y} \boldsymbol{C}_i(\boldsymbol{\theta}, \boldsymbol{y}^0)(y_i - y^0_i), \tag{22}$$

where $\boldsymbol{y}^0$ denotes the expected value of $\boldsymbol{Y}$; y^0_i is the i-th component of $\boldsymbol{y}^0$; n_y denotes the number of components of the random variable vector $\boldsymbol{Y}$; $\overline{\boldsymbol{c}}_0$ and $\boldsymbol{C}_0$ denote the vector $\overline{\boldsymbol{c}}$ and matrix $\boldsymbol{C}$ evaluated at $(\boldsymbol{\theta}, \boldsymbol{y}^0)$, respectively; and $\overline{\boldsymbol{c}}_i$ and $\boldsymbol{C}_i$ denote the partial derivative of vector $\overline{\boldsymbol{c}}$ and matrix $\boldsymbol{C}$ with respect to y_i evaluated at $(\boldsymbol{\theta}, \boldsymbol{y}^0)$, respectively, that is:

$$\overline{\boldsymbol{c}}_i(\boldsymbol{\theta}, \boldsymbol{y}^0) = \left. \frac{\partial \overline{\boldsymbol{c}}(\boldsymbol{\theta}, \boldsymbol{y})}{\partial y_i} \right|_{\boldsymbol{y}=\boldsymbol{y}^0},\ i = 1, \ldots, n_y \tag{23}$$

$$\boldsymbol{C}_i(\boldsymbol{\theta}, \boldsymbol{y}^0) = \left. \frac{\partial \boldsymbol{C}(\boldsymbol{\theta}, \boldsymbol{y})}{\partial y_i} \right|_{\boldsymbol{y}=\boldsymbol{y}^0},\ i = 1, \ldots, n_y. \tag{24}$$

Note that the latter derivatives can be obtained by analytical or numerical approaches (for example, finite differences), as discussed in [30]. The approximation proposed in Eq. (22) should provide reasonable results when the uncertainty associated with $\boldsymbol{Y}$ is relatively small. In practical applications pertaining, e.g. structural systems, such assumption may be reasonable.

Let $\boldsymbol{d}_i,\ i=0,\dots,n_y$ denote a vector of dimension n_r. The j-th component of this vector (which is denoted as $(d_j)_i$) is defined such that:

$$(d_j)_i(\boldsymbol{\theta},\boldsymbol{y}^0)=\sum_{k=1}^{n_z}\left((c_{j,k})_i(\boldsymbol{\theta},\boldsymbol{y}^0)\right)^2,\ j=1,\dots,\boldsymbol{n_r},\ i=0 \tag{25}$$

$$(d_j)_i(\boldsymbol{\theta},\boldsymbol{y}^0)=\left((\overline{c}_j)_i(\boldsymbol{\theta},\boldsymbol{y}^0)\right)^2+\sum_{k=1}^{n_z}\left((c_{j,k})_i(\boldsymbol{\theta},\boldsymbol{y}^0)\right)^2,\ j=1,\dots,\boldsymbol{n_r},\ i=1,\dots,n_y, \tag{26}$$

where $(\overline{c}_j)_i$ is the j-th entry of vector $\overline{\boldsymbol{c}}_i$ and $(c_{j,k})_i$ is the element of the j-th row and k-th column of matrix $\boldsymbol{C}_i$. Then, it is straightforward to show that the maximum standard deviation can be approximated as:

$$\sigma_{\max}(\boldsymbol{\theta})\approx\sigma_{\max}^L(\boldsymbol{\theta})=\sqrt{\|\boldsymbol{d}_0(\boldsymbol{\theta},\boldsymbol{y}^0)+\sum_{i=1}^{n_y}\boldsymbol{d}_i(\boldsymbol{\theta},\boldsymbol{y}^0)\mathcal{V}[y_i]\|_\infty}, \tag{27}$$

where $\sigma_{\max}^L(\boldsymbol{\theta})$ denotes the approximate maximum standard deviation and $\mathcal{V}[y_i]$ denotes variance of the i-th random variable Y_i. It is emphasized that the calculation of vectors $\boldsymbol{d}_i,\ i=0,\dots,n_y$ does not involve any random sampling; hence, they can be efficiently determined by performing deterministic structural analysis. Furthermore, Eq. (27) provides a precise value which is more amenable for optimization than an estimator.

As a summary of the above discussion, the proposed approach for bounding the failure probability of a structural system affected by aleatoric and epistemic uncertainties consists of the following two steps. The first step involves the approximate standard deviation provided in Eq. (27), that is considered for solving the optimization problems in Eqs. (14, 15). This allows to identify the crisp values of the epistemic parameters that lead to a minimum/maximum value of the failure probability. Note that the solution of these optimization problems involves dealing explicitly with epistemic uncertainty only, as the aleatoric uncertainty is implicitly considered with the closed-form approximation of the standard deviation provided by Eq. (27). Then, the second step involves calculating the failure probability for the crisp values of the epistemic parameters previously identified by performing, e.g. simulation with respect to the aleatoric uncertain parameters. This allows estimating the sought bounds for the probability. The advantage of the proposed approach is that the classic double-loop approach for propagating epistemic and aleatoric uncertainty is effectively broken, as the first step (optimization with respect to maximum standard deviation) addresses the effect of epistemic uncertainty while the second step deals with aleatoric uncertainty.

4. Examples

The following engineering examples show that the standard deviation is a good proxy of the failure probability. The first example is a clamped plate subjected to loading modeled as a random field. Then a single-degree-of-freedom oscillator subject to stochastic ground acceleration and a three-story concrete frame subjected to a stochastic wind load are presented. These two examples from structural dynamics show a strong nonlinear behavior of the first excursion probability with respect to epistemic uncertain parameters. The functionality of the presented method in such cases is demonstrated. A comparison of the proposed approach (decoupled approach based on the maximum standard deviation) and a direct optimization approach with a double loop algorithm is provided. For the direct optimization, a classical Monte Carlo simulation (MCS) and alternatively Directional Importance Sampling (DIS) from [31, 32] are used to estimate the failure probability $p_F(\boldsymbol{\theta})$. The performed optimization procedure to find the extreme values $\underline{\theta}^*$ and $\overline{\theta}^*$ of the failure probability for both approaches is depicted in Figure 1 . No optimization-based interval analysis

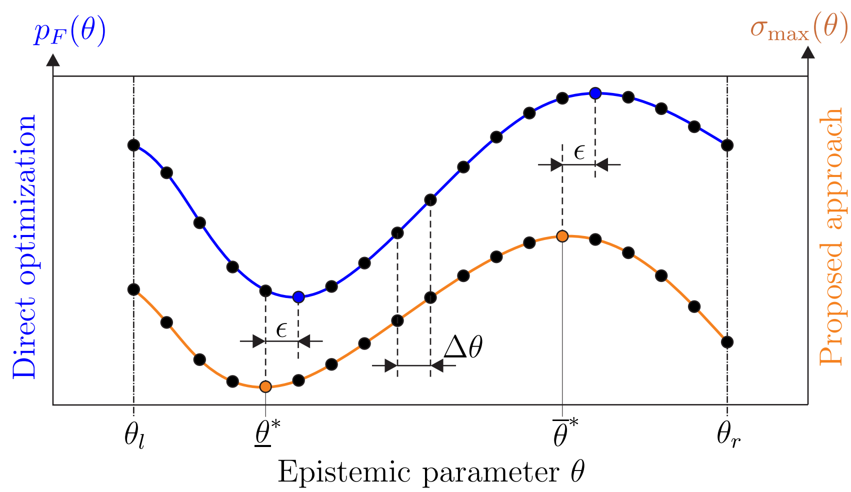

Figure 1: Optimization procedure to find the extreme values $\underline{\theta}^*$ and $\overline{\theta}^*$ of the failure probbaility

is performed, where an efficient optimization algorithm is used to find the extreme values. For comparison of the relative execution time the examined epistemic parameter $\theta = [\theta_l, \theta_r]$ is discretized in equal increments $\Delta\theta = \frac{\theta_r - \theta_l}{N_e - 1}$. This means, for each approach (proposed and direct) a total number of N_e simulations are performed. In addition, the error ϵ as shown in Figure 1 between the extreme values calculated by both approaches is evaluated.

4.1. Plate subjected to random loading

First a clamped plate subjected to random loading is investigated, see Figure 2. The finite

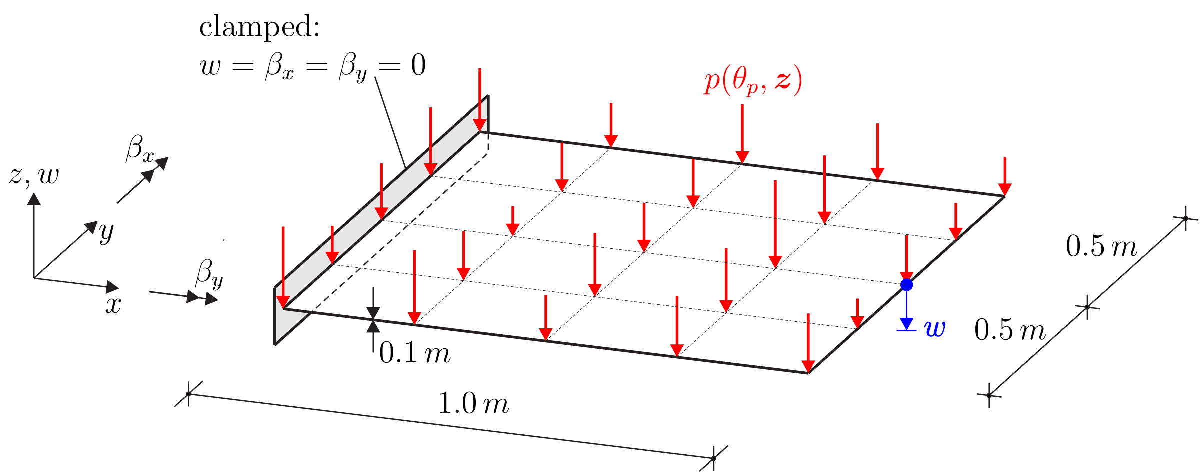

Figure 2: Clamped plate subjected to stochastic loading

element model is discretized with 20×20 geometrical linear quadrilateral shell elements based on the Reissner–Mindlin theory. The plate is moderately thick with dimensions $l_x = l_y = 1.0\,m$ and a thickness of $t = 0.1\,m$. A concrete material is simulated with a Poisson's ratio of $\nu = 0.2$, where the Young's modulus E is assumed to be a (truncated) Gaussian variable defined as follows

$$E = \mathcal{N}(\mu_E = 3.3 \cdot 10^7\,kN/m^2, \sigma_E = 0.1 \cdot \mu_E). \tag{28}$$

The surface load $p(\boldsymbol{\theta}_p, \boldsymbol{z})$ according to Eq. (1) is modeled by a Gaussian random field with a non-zero mean $\mu = 0.2\,kN$. Thereby, a homogeneous correlation function is defined as follows

$$C(\tau) = \sigma^2 \rho(\tau). \tag{29}$$

The standard deviation is $\sigma = 0.03\,kN$ and for the autocorrelation function $\rho(\tau)$ the quadratic exponential form

$$\rho(\tau) = \exp\left[-\frac{\tau^2}{\ell_c^2}\right] \tag{30}$$

is used, where τ represents the distance between two points of the plate. The epistemic part of the example is described by the correlation length as an interval variable $\theta_p = \ell_c = [0.25, 1.0]\ m$. The distribution of the load over space $p_{\boldsymbol{z}}(x, y)$ depends highly on the correlation length. Therefore, two random field realizations for the interval bounds are depicted in Figure 3.

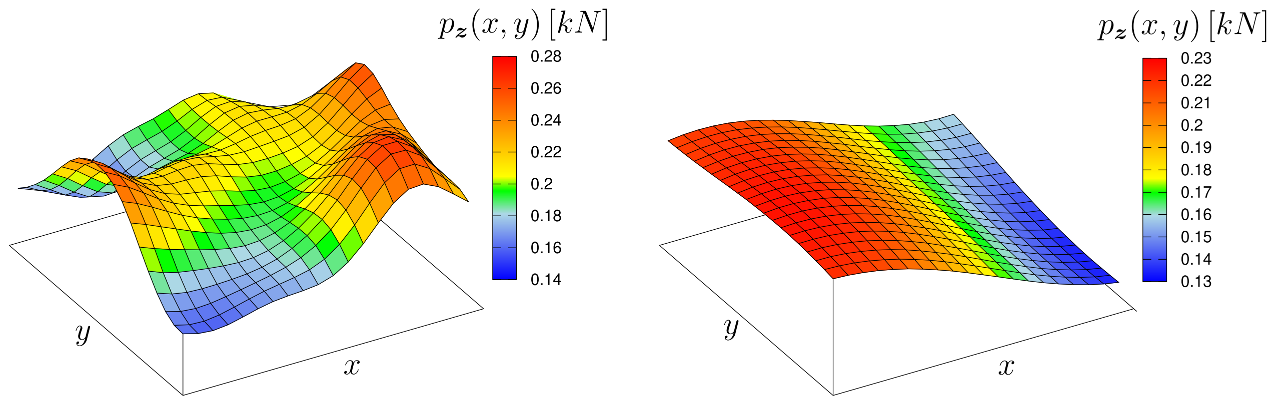

Figure 3: Random field realizations of the load $p_{\boldsymbol{z}}(x, y)$ for the interval bounds of the correlation length: $\ell_c = 0.25$ (left) and $\ell_c = 1.0$ (right)

The random field is generated by the Karhunen-Loève expansion (KLE), where the number of random field nodes $n_r = 21 \times 21 = 441$ is equal to the number of the finite element nodes. The number of retained terms n_{KL} for the KLE depends on the correlation length and is determined when the sum of eigenvalues exceeds 99% of the total amount. The objective of the problem is to calculate the bounds of the exceedance probability of the displacement w, where the displacement should not exceed the threshold of $0.005\,m$. The maximum standard deviation $\sigma_{\max}$ and the probability of failure $p_F(\ell_c)$ versus the correlation length ℓ_c are shown in Figure 4. For comparison, the proposed $\sigma_{\max}(\ell_c)$ and the direct optimization approach based on the MCS to calculate $p_F(\ell_c)$ is evaluated on $N_e = 20$ equidistant points within the interval $\ell_c = [0.25, 1.0]$. On each point a MCS is performed with 10^5 simulations. This means, the FE-model is evaluated $10^5 \times 20 = 2 \times 10^6$ times. A monotonic behavior can be observed for both curves. Not always such behavior can be predicted. In this case, the greater the correlation length the greater the probability of failure. If the loads scatter very strongly (small correlation length), a balancing effect can be observed.

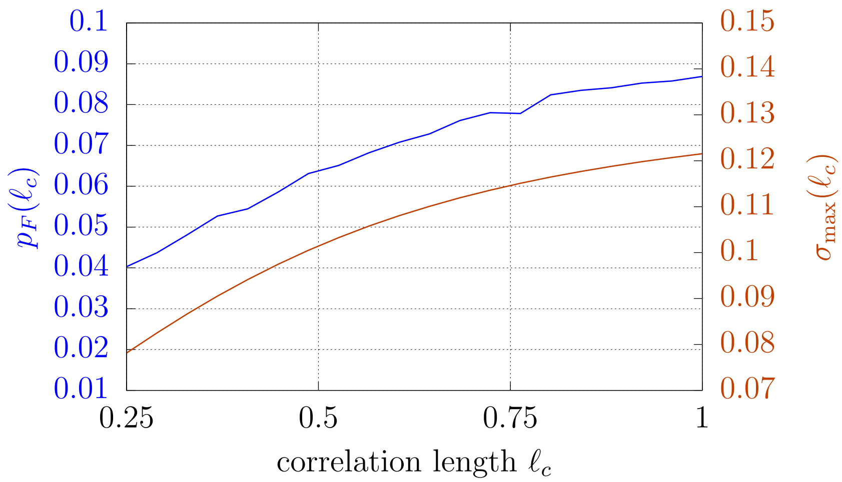

Figure 4: Maximum standard deviation $\sigma_{\max}(\ell_c)$ and failure probability ($p_F(\ell_c)$) versus the correlation length ℓ_c.

For example, a large point load on a specific node can be directly compensated by a small point load on the neighbor node. This is not possible for a smooth field (large correlation length). It is noted that if a monotonic behavior can be estimated, no optimization is needed and a simulation can be performed directly on the interval bounds. The results of the failure probability bounds for both approaches are shown in Table 1.

	Proposed approach		Direct optimization (MCS)	
	lower bound	upper bound	lower bound	upper bound
p_F	7.82×10^{-2}	12.15×10^{-2}	4.03×10^{-2}	8.69×10^{-2}
ℓ_c [m]	0.25	1.00	0.25	1.00
Relative execution time	1		3873	

Table 1: Bounds of failure probability for the plate subjected to stochastic loading

The relative execution time is reduced from 3873 to 1 using the proposed approach, which clearly demonstrates its advantage. Also if a more efficent optimization-based interval analysis is applied, where less than the 20 MCS are required, the proposed approach can be still faster compared to the double-loop approach.

4.2. Single-degree-of-freedom oscillator subject to stochastic ground acceleration

This example consists of a single-degree-of-freedom oscillator subjected to a stochastic ground acceleration, as depicted schematically in Figure 5. The mass of the oscillator is characterized as a random variable while its stiffness is described by means of an interval-valued variable. The objective of the problem is to calculate the bounds of the first excursion probability.

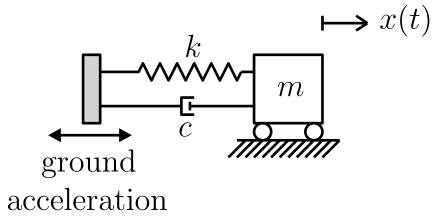

Figure 5: Single-degree-of-freedom oscillator subject to stochastic ground acceleration.

The stochastic ground acceleration possesses a time duration $T = 20$ [s] and follows a modulated Clough-Penzien spectrum (see, e.g. [33, 34]). The spectrum is implemented considering spectral intensity of 5×10^{-3} [m^2/s^3], natural circular frequencies of 6π [rad/s] and 0.6π [rad/s] for the primary and secondary filters, respectively, and damping ratios of 60%. The modulation function follows the Shinozuka-Sato model with shape parameters $c_1 = 0.14$ and $c_2 = 0.16$ [35]. The spectrum is represented considering a time step discretization $\Delta t = 0.05$ [s] by means of the well-known Karhunen-Loève expansion, retaining 99% of the total variability, leading to $n_z = 361$ terms.

The stiffness k of the oscillator is modeled as an interval variable such that $k = \theta_1 = [70, 470]$ [N/m]. The mass $m = y_1$ follows a lognormal distribution with expected value 1 [kg] and coefficient of variation of δ_m (the numerical value of this coefficient is discussed later in this example). The model possesses classical damping $c = 5\%$. Two responses of interest are to be controlled within the duration of the stochastic ground acceleration: the relative displacement and the absolute acceleration of the oscillator. None of these responses should exceed the thresholds of 7 [cm] and 7.5 [m/s^2], respectively. As the total duration of the ground acceleration is 20 [s] and time is discretized at steps of 0.05 [s], the number of responses to be controlled is equal to $n_r = (20/0.05 + 1) \times 2 = 802$.

Recall that the objective is to estimate the bounds of the first excursion probability associated with the oscillator. Nonetheless, before proceeding with such calculation, the quality of the approximate expression for the maximum standard deviation (see Eq. (27)) is evaluated. Figure 6 shows the estimated maximum standard deviation as a function of the stiffness for the cases where the coefficient of variation of the mass is equal to $\delta_m = 2\%$ and $\delta_m = 10\%$. In each of the two plots, the approximate standard deviation $\sigma^L_{\max}$ as calculated by means of Eq. (27) is plotted against the reference value $\sigma^S_{\max}$ as obtained by performing $N_e = 100$ simulations (that is, per each value of the stiffness k considered, 100 samples of the mass m are drawn, see Eq. (19)). It is noted that for the case where $\delta_m = 2\%$, there is a very good agreement between the approximate and reference results. Contrary, for the case where $\delta_m = 10\%$, there are considerable differences between approximate and reference results. This was expected as the linearization strategy considered for calculating the approximate maximum standard deviation loses accuracy as the coefficient of variation of the mass increases. Despite these differences, it should be noted that the minimum and maximum values of these two curves occur for similar values of the stiffness. This is quite relevant, as one is interested in locating which values of the epistemic parameter (in this case, the stiffness k) produce the minimum and maximum value of the standard deviation, while the value of the standard deviation itself is less important.

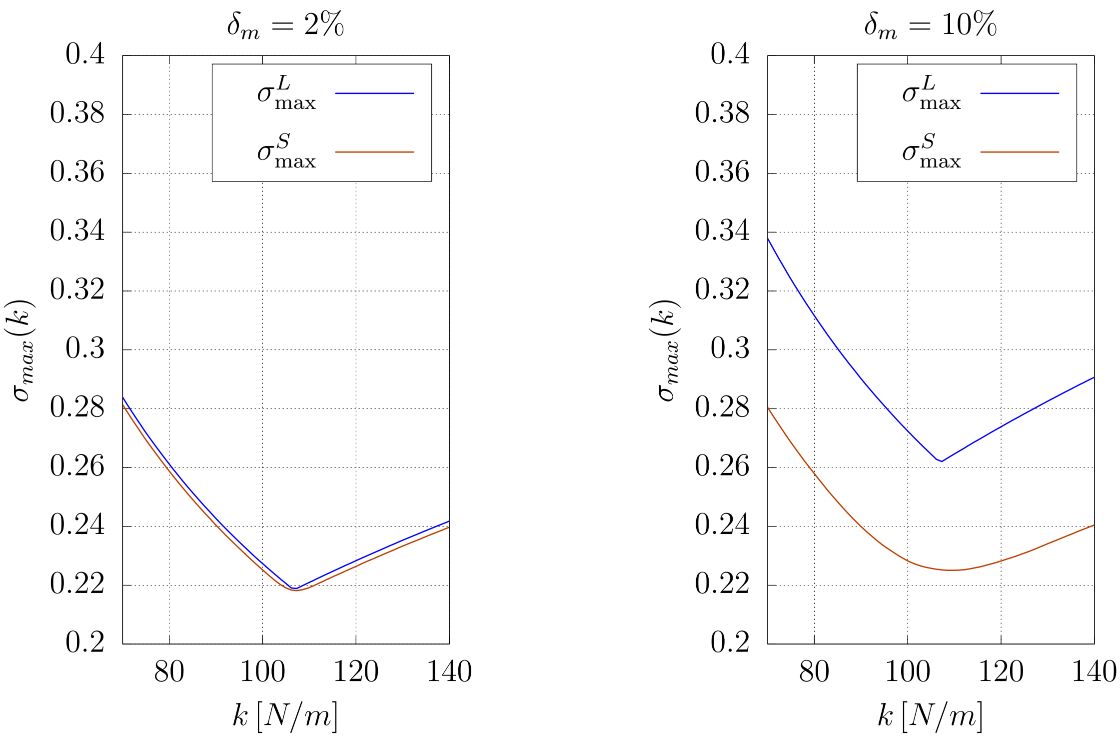

Figure 6: Maximum standard deviation ($\sigma_{\max}$) as a function of the stiffness (k).

The next step is calculating the bounds of the failure probability. For doing so, the coefficient of variation of the mass is set equal to $\delta_m = 10\%$. The bounds for the failure probability are obtained by means of:

- Proposed approach. That is, optimization is applied to identify the value of the epistemic parameter $k = \theta_1$ that minimizes (maximizes) the approximate maximum standard deviation $\sigma^L_{\max}$. Then, for the identified values of k, the bounds of the failure probability are obtained by performing two separate Monte Carlo simulation runs.

- Direct optimization. That is, the bounds of the failure probability are obtained by directly minimizing (maximizing) the probability value obtained by means of optimization-based interval analysis and Monte Carlo simulation.

As the system under consideration is linear and is subjected to Gaussian acceleration, the failure probability is estimated by means of Directional Importance Sampling [31, 32]. To ensure sufficiently accurate estimators of the failure probability, Directional Importance Sampling is implemented considering a total of 2000 samples. That is, to generate an estimate of the failure probability, it is necessary to perform 2000 dynamic analyses. The results obtained when applying the proposed and direct approaches are shown in Table 2. As noted from this table, the proposed approach offers quite accurate estimates of the bounds of the failure probability when compared with the direct approach. In fact, both approaches produce identical results for the estimate of the upper bound for the failure probability while there are small differences regarding the lower bound. Moreover, there is a huge gain regarding computation time, as the proposed approach is 64.9 times faster than the direct one.

	Proposed approach		Direct optimization (DIS)	
	lower bound	upper bound	lower bound	upper bound
p_F	4.6×10^{-3}	1.5×10^{-2}	4.4×10^{-3}	1.5×10^{-2}
k [N/m]	107	70	111	70
Relative execution time	1		64.9	

Table 2: Bounds of failure probability for single-degree-of-freedom oscillator example

A deeper understanding of the results presented in Table 2 can be achieved by means of Figure 7, that illustrates the failure probability (p_F) and the maximum standard deviation calculated using the linear approximation ($\sigma^L_{\max}$, see Eq. (27)) and simulation ($\sigma^S_{\max}$) as a function of the stiffness k. It is readily noticed that maximum standard deviation offers an excellent proxy for locating the minimum and maximum values of the failure probability, even though there is a small offset regarding the value of the stiffness that leads to the lower bound failure probability, as already noted in Table 2.

4.3. Three-story concrete frame subjected to a stochastic wind load

A three-story concrete frame taken from [36] is modeled as a three-mass oscillator. The presented approach based on the maximum standard deviation is intended to reduce computing times in such simulations significantly. Moreover, the objective of this example is to show that the bounds can also be identified for more complex behaviors of the first excursion probability.

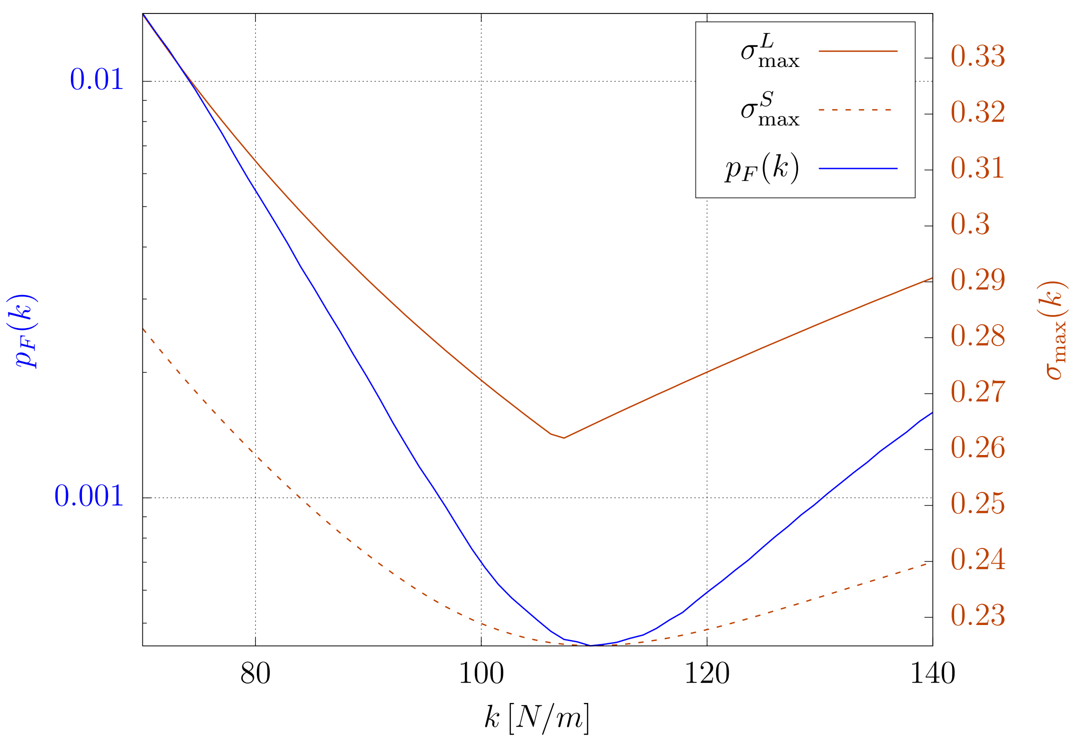

Figure 7: Maximum standard deviation $\sigma_{\max}$ and failure probability ($p_F(k)$) versus stiffness (k).

The simplified model of the three-story concrete frame with a stochastic wind load $F(t)$ is depicted in Figure 8. The concrete floors are modeled as rigid bars. Dead and traffic loads are fully considered in the point masses which are characterized as (truncated) Gaussian random variables. The expected value and standard deviation of the masses $y_1 = m_1 = m_2$ hold $\mu = 9500\,kg$ and $\sigma = 950\,kg$. The mass of the top floor $y_2 = m_3$ is slightly lower than the others with $\mu = 9000\,kg$ and $\sigma = 900\,kg$. For bending stiffness of the concrete columns an interval-valued variable $k = \theta_1 = [1000, 7000]\,kN/m$ is defined. The damping of the model is neglected. On the top of the frame a stochastic wind load is simulated with the homogeneous correlation function defined in Eq. (29). The variance is specified with $\sigma^2 = 400\,kN^2$ and the autocorrelation function to simulate a realistic wind loading is defined as follows

$$\rho(\tau) = \cos(A\sqrt{1 - B^2}\,\tau)\exp(-C\,\tau) \quad \text{with} \quad A = 30, B^2 = 0.05 \text{ and } C = 0.3, \tag{31}$$

where τ represents the time lag. The autocorrelation function given by Eq. (31) is shown in Figure 9. The stochastic process of the wind loading with a total duration $T = 10\,s$ is represented considering a time step discretization $\tau = 0.01\,s$ by means of the Karhunen-Loève expansion. The number of responses to be controlled is equal to $n_r = (10/0.01 + 1) = 1001$. A truncation of the

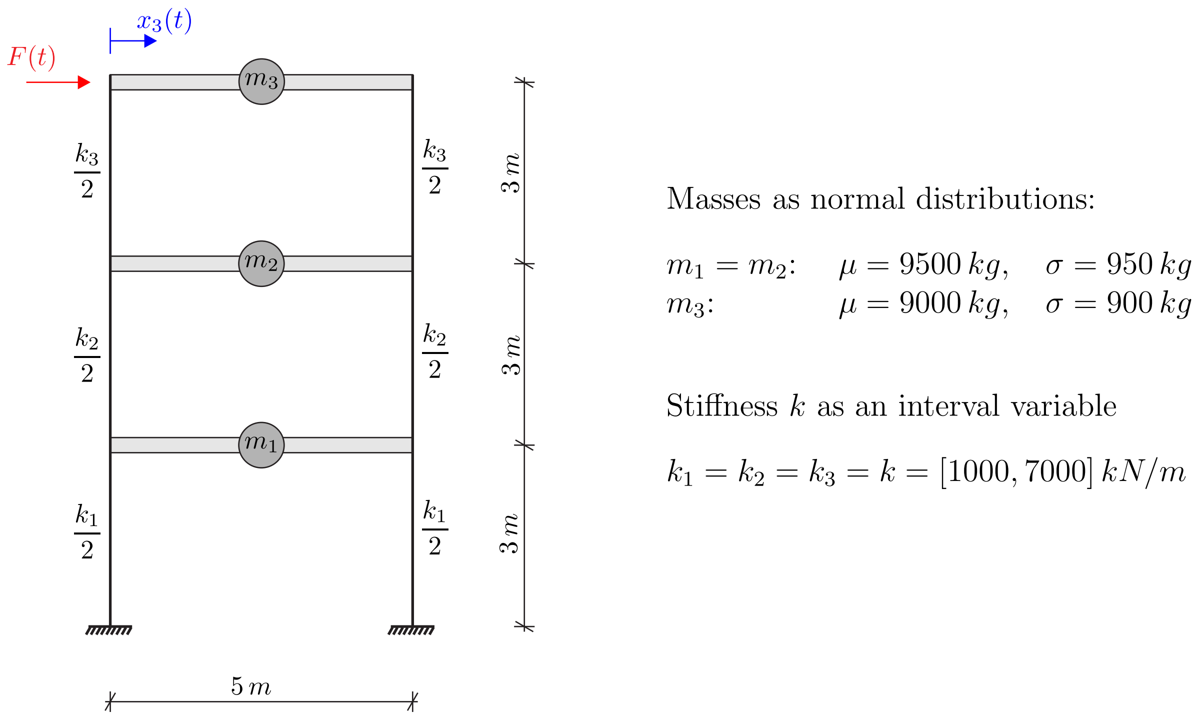

Figure 8: Three-degree-of-freedom model of the concrete frame

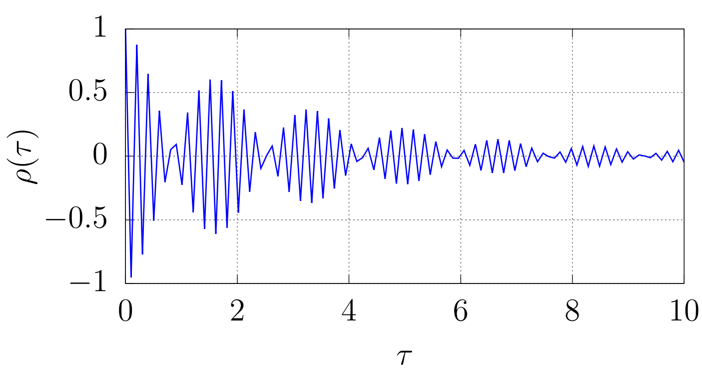

Figure 9: Autocorrelation function to simulate a stochastic wind load.

series is performed when the sum of eigenvalues exceeds 99% of the total amount. This means $n_{KL} = 111$ terms have to be used. The response of interest within the duration of the stochastic wind process is the top displacement $x_3(t)$. In the duration the threshold value $x_3(t) = 0.02\,m$ should not be exceeded. The results of the failure probability $p_F(k)$ and the maximum standard deviation $\sigma_{\max}(k)$ are shown in Figure 10. For the proposed and the direct optimization approach based on the MCS to calculate $p_F(k)$ the epistemic parameter k is discretized on $N_e = 200$ points. To calculate $p_f(k)$ a MCS is performed with 10^4 samples. This means, the model is evaluated 2×10^6 times. It is interesting to note that two maxima of the failure probability can be observed with increasing stiffness. The extreme values of $\sigma_{\max}(k)$ correlate with a small approximation

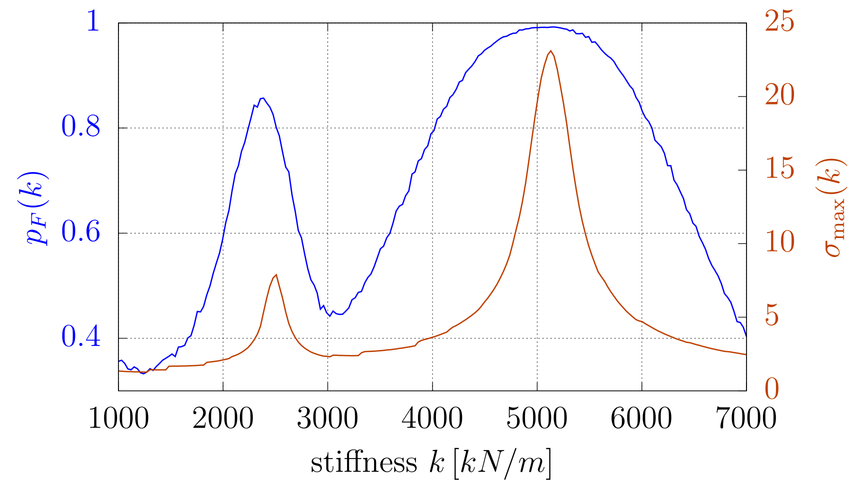

Figure 10: Maximum standard deviation $\sigma_{\max}(k)$ and failure probability $p_F(k)$ versus stiffness k.

failure with those of the function $p_F(k)$, see Table 3. In this example the approach based on the

	Proposed approach		Direct optimization (MCS)	
	lower bound	upper bound	lower bound	upper bound
p_F	0.3358	0.9921	0.3324	0.9923
k [N/m]	1271.4	5130.7	1241.2	5160.8
Relative computation time	1		1463	

Table 3: Bounds of failure probability for three-story concrete frame subjected to a stochastic wind load

maximum standard deviation is 1463 times faster than the double-loop Monte Carlo simulation.

5. Conclusions and Outlook

The proposed approach aims to estimate approximately the bounds of the failure probability for linear structural systems subject to epistemic and aleatoric uncertainty. For different engineering applications such as a clamped concrete plate, a single-degree-of-freedom oscillator and a three-story concrete frame the proposed approach is presented and compared with common sampling methods. With the presented results it is shown that the maximum standard deviation of the response of a model serves as an excellent proxy for determining the bounds of the failure probability. The approximate approach based on the maximum standard deviation can be used to replace a classical double-loop approach for computing the probability bounds with a decoupled approach. The numerical examples indicate that such replacement may lead to reduce the numerical effort significantly without sacrificing accuracy in the estimates of the bounds.

While the results presented are promising, only linear systems can be approximated. An idea for further research is to integrate the presented approach in the concept of polymorphic/hybrid uncertainties, where more than one epistemic parameter is considered. If at least one parameter is described as a fuzzy number, a computationally expensive α-level optimization has to be performed. The aim is to reduce the computational effort in such concepts significantly. Another path for future research efforts consists of extending the application of the proposed approach to problems involving a considerable number of epistemic parameters. In principle, such extension should be feasible according to results discussed in [17].

Appendix A. Response Calculation

This contribution assumes that the response of a structural system can be cast as described in Eq. (3). This appendix illustrates how such assumption would apply to a linear system under static and dynamic loading, respectively.

First, consider a linear structural system subject to static loading. For simplicity, it is assumed that the number of degrees-of-freedom of the system is n_f, which is the dimension of the force vector. The displacement of the system is (see, e.g. [25, 37]):

$$\boldsymbol{\eta}^* = \boldsymbol{K}^{-1}\boldsymbol{f}. \tag{A.1}$$

where $\boldsymbol{K}$, $\boldsymbol{f}$ and $\boldsymbol{\eta}^\star$ correspond to stiffness matrix (of dimension $n_f \times n_f$), load and displacement vectors (each of dimension $n_f \times 1$), respectively. It is observed that the inverse of the stiffness matrix corresponds to matrix $\boldsymbol{A}$ appearing in Eq. (3).

Second, consider a linear elastic system under dynamic loading. For simplicity, consider a single-degree-of-freedom system subject to a (possibly imprecise) Gaussian loading whose discrete time representation comprises n_f points. Furthermore, assume that the response of interest is the displacement at each time instant. Then, the response of interest at the k-th time instant can be calculated by means of a convolution integral, that is [38]:

$$\eta_k^* = \int_0^{t_k} h(t_k - \tau) f(\tau) d\tau,\ k = 1, \ldots, n_f, \tag{A.2}$$

where h denotes the impulse response function. Using an appropriate quadrature scheme [39], this convolution integral can be approximated as:

$$\eta_k^* = \boldsymbol{h}_k \boldsymbol{f},\ k = 1, \ldots, n_f, \tag{A.3}$$

where $\boldsymbol{h}_k$ is a $1 \times n_f$ vector whose coefficients depend on the quadrature ruled considered and the impulse response function evaluated at different time instants. From Eq. (A.3), it can be noted that the response vector $\boldsymbol{\eta}^*$ can be expressed in this case as:

$$\boldsymbol{\eta}^* = \begin{bmatrix} \boldsymbol{h}_1 \\ \boldsymbol{h}_2 \\ \vdots \\ \boldsymbol{h}_{n_f} \end{bmatrix} \boldsymbol{f}, \tag{A.4}$$

where the matrix collecting the row vectors $\boldsymbol{h}_k,\ k = 1, \ldots, n_f$ would correspond to matrix $\boldsymbol{A}$ in Eq. (3).

It is emphasized that the different expressions shown in this Appendix were deduced following simplifying assumptions. This is justified as the aim is illustrating how Eq. (3) is able to describe the behavior of linear structures under static or dynamic loading. For more general cases, it is referred to, e.g. [25, 38, 40].

Appendix B. Operator Norm Framework: Analysis for the case of p^1=∞ and $p^2 = 2$

According to [29], the operator norm associated with matrix $\boldsymbol{D}(\boldsymbol{\zeta})$ for the case where p^1=∞ and $p^2 = 2$ is equal to the maximum Euclidean norm of a row of that matrix. That is:

$$||\boldsymbol{D}(\boldsymbol{\zeta})||_{p^1,p^2} = \max_{k=1,\ldots,d_r} \left(\sqrt{\boldsymbol{d}_k(\boldsymbol{\zeta})\boldsymbol{d}_k(\boldsymbol{\zeta})^T} \right), \tag{B.1}$$

where $\boldsymbol{d}_k(\boldsymbol{\zeta})$ is the k-th row of matrix $\boldsymbol{D}(\boldsymbol{\zeta})$. In order to understand the physical meaning of this operator norm, consider the k-th component of $\boldsymbol{\xi}$ (denoted as ξ_k), which is calculated as:

$$\xi_k(\boldsymbol{\zeta}) = \boldsymbol{d}_k(\boldsymbol{\zeta})\boldsymbol{v}. \tag{B.2}$$

Then, assuming that vector $\boldsymbol{v}$ is a realisation of a multivariate standard Gaussian distribution (that is, zero mean and unit standard deviation, see Section 2.2), it is noted that the expected value and variance of ξ_k are given by:

$$\mathcal{E}\left[\xi_k\right] = \mathcal{E}\left[\boldsymbol{d}_k\boldsymbol{v}\right] = \boldsymbol{d}_k\mathcal{E}\left[\boldsymbol{v}\right] = 0 \tag{B.3}$$

$$\mathcal{V}\left[\xi_k\right] = \mathcal{E}\left[(\xi_k - \mathcal{E}\left[\xi_k\right])^2\right] = \mathcal{E}\left[(\boldsymbol{d}_k\boldsymbol{v})^2\right] = \boldsymbol{d}_k\mathcal{E}\left[\boldsymbol{v}\boldsymbol{v}^T\right]\boldsymbol{d}_k^T = \boldsymbol{d}_k\boldsymbol{d}_k^T, \tag{B.4}$$

where $\mathcal{E}$ denotes expectation and $\mathcal{V}$ variance. From Eq. (B.4), it is observed that the quantity $\sqrt{\boldsymbol{d}_k \boldsymbol{d}_k^T}$ is the standard deviation of ξ_k. This implies that the operator norm as shown in Eq. (B.1) actually returns the maximum standard deviation of vector $\boldsymbol{\xi}$.

References

[1] G. Stefanou, The stochastic finite element method: Past, present and future, Computer Methods in Applied Mechanics and Engineering 198 (9-12) (2009) 1031–1051.

[2] M. Faes, D. Moens, Recent trends in the modeling and quantification of non-probabilistic uncertainty, Archives of Computational Methods in Engineering 27 (3) (2020) 633–671. doi:10.1007/s11831-019-09327-x.

[3] C. Jiang, J. Zheng, X. Han, Probability-interval hybrid uncertainty analysis for structures with both aleatory and epistemic uncertainties: a review, Structural and Multidisciplinary Optimization 57 (6) (2018) 2485–2502. doi:10.1007/s00158-017-1864-4.

[4] W. Graf, M. Götz, M. Kaliske, Analysis of dynamical processes under consideration of polymorphic uncertainty, Structural Safety 52, Part B (2015) 194–201, Engineering Analyses with Vague and Imprecise Information. doi:10.1016/j.strusafe.2014.09.003.

[5] M. Beer, S. Ferson, V. Kreinovich, Imprecise probabilities in engineering analyses, Mechanical Systems and Signal Processing 37 (1-2) (2013) 4–29. doi:10.1016/j.ymssp.2013.01.024.

[6] M. Faes, M. Daub, S. Marelli, E. Patelli, M. Beer, Engineering analysis with probability boxes: A review on computational methods, Structural Safety 93 (2021) 102092. doi:10.1016/j.strusafe.2021.102092.

[7] D. Moens, D. Vandepitte, An interval finite element approach for the calculation of envelope frequency response functions, International Journal for Numerical Methods in Engineering 61 (14) (2004) 2480–2507. doi:10.1002/nme.1159.

[8] P. Wei, J. Song, S. Bi, M. Broggi, M. Beer, Z. Lu, Z. Yue, Non-intrusive stochastic analysis with parameterized imprecise probability models: I. performance estimation, Mechanical Systems and Signal Processing 124 (2019) 349 – 368. doi:10.1016/j.ymssp.2019.01.058.

[9] R. Schöbi, B. Sudret, Structural reliability analysis for p-boxes using multi-level meta-models, Probabilistic Engineering Mechanics 48 (2017) 27–38. doi:10.1016/j.probengmech.2017.04.001.

[10] M. Fina, P. Weber, W. Wagner, Polymorphic uncertainty modeling for the simulation of geometric imperfections in probabilistic design of cylindrical shells, Structural Safety 82 (2020) 101894. doi:10.1016/j.strusafe.2019.101894.

[11] S. Freitag, P. Edler, K. Kremer, G. Meschke, Multilevel surrogate modeling approach for optimization problems with polymorphic uncertain parameters, International Journal of Approximate Reasoning 119 (2020) 81–91. doi:10.1016/j.ijar.2019.12.015.

[12] P. Wei, F. Liu, M. Valdebenito, M. Beer, Bayesian probabilistic propagation of imprecise probabilities with large epistemic uncertainty, Mechanical Systems and Signal Processing 149 (2021) 107219. doi:10.1016/j.ymssp.2020.107219.

[13] C. Dang, P. Wei, J. Song, M. Beer, Estimation of failure probability function under imprecise probabilities by active learning–augmented probabilistic integration, ASCE-ASME Journal of Risk and Uncertainty in Engineering Systems, Part A: Civil Engineering 7 (4) (2021) 04021054. doi:10.1061/AJRUA6.0001179.

[14] M. de Angelis, E. Patelli, M. Beer, Advanced Line Sampling for efficient robust reliability analysis, Structural Safety 52, Part B (2015) 170–182. doi:10.1016/j.strusafe.2014.10.002.

[15] J. Hurtado, D. Alvarez, J. Ramirez, Fuzzy structural analysis based on fundamental reliability concepts, Computers & Structures 112–113 (2012) 183–192. doi:10.1016/j.compstruc.2012.08.004.

[16] M. Troffaes, Imprecise Monte Carlo simulation and iterative importance sampling for the estimation of lower previsions, International Journal of Approximate Reasoning 101 (2018) 31 – 48. doi:10.1016/j.ijar.2018.06.009.

[17] M. Faes, M. Valdebenito, Fully decoupled reliability-based design optimization of structural systems subject to uncertain loads, Computer Methods in Applied Mechanics and Engineering 371 (2020) 113313. doi:doi.org/10.1016/j.cma.2020.113313.

[18] M. Faes, M. Valdebenito, D. Moens, M. Beer, Bounding the first excursion probability of linear structures subjected to imprecise stochastic loading, Computers & Structures 239 (2020) 106320. doi:10.1016/j.compstruc.2020.106320.

[19] M. Faes, M. Valdebenito, D. Moens, M. Beer, Operator norm theory as an efficient tool to propagate hybrid uncertainties and calculate imprecise probabilities, Mechanical Systems and Signal Processing 152 (2021) 107482. doi:10.1016/j.ymssp.2020.107482.

[20] P. Ni, D. Jerez, V. Fragkoulis, M. Faes, M. Valdebenito, M. Beer, Operator norm-based statistical linearization to bound the first excursion probability of nonlinear structures subjected to imprecise stochastic loading, ASCE-ASME Journal of Risk and Uncertainty in Engineering Systems, Part A: Civil Engineering 8 (1) (2022) 04021086. doi:10.1061/AJRUA6.0001217.

[21] F. Leichsenring, C. Jenkel, W. Graf, M. Kaliske, Numerical simulation of wooden structures with polymorphic uncertainty in material properties, International Journal of Reliability and Safety 12 (1–2) (2018) 24–45. doi:10.1056/NEJMoa1716816.

[22] M. Beer, Y. Zhang, S. Quek, K. Phoon, Reliability analysis with scarce information: Comparing alternative approaches in a geotechnical engineering context, Structural Safety 41 (2013) 1–10. doi:10.1016/j.strusafe.2012.10.003.

[23] T. Soong, M. Grigoriu, Random Vibration of Mechanical and Structural Systems, Prentice Hall, Englewood Cliffs, New Jersey, 1993.

[24] C. Schenk, G. Schuëller, Uncertainty Assessment of Large Finite Element Systems, Springer-Verlag, Berlin/Heidelberg/New York, 2005.

[25] K. Bathe, Finite Element Procedures, Prentice Hall, New Jersey, 1996.

[26] S. Au, J. Beck, Estimation of small failure probabilities in high dimensions by subset simulation, Probabilistic Engineering Mechanics 16 (4) (2001) 263–277.

[27] M. Faes, M. Valdebenito, D. Moens, M. Beer, Operator norm theory as an efficient tool to propagate hybrid uncertainties and calculate imprecise probabilities, Mechanical Systems and Signal Processing 152 (2021) 107482. doi:10.1016/j.ymssp.2020.107482.

[28] M. Faes, M. Valdebenito, Fully decoupled reliability-based optimization of linear structures subject to Gaussian dynamic loading considering discrete design variables, Mechanical Systems and Signal Processing 156 (2021) 107616. doi:10.1016/j.ymssp.2021.107616.

[29] J. Tropp, Topics in sparse approximation, Ph.D. thesis, The University of Texas at Austin (2004).

[30] R. Haftka, Z. Gürdal, Elements of Structural Optimization, 3^{rd} Edition, Kluwer, Dordrecht, The Netherlands, 1992.

[31] O. Ditlevsen, P. Bjerager, R. Olesen, A. Hasofer, Directional simulation in Gaussian processes, Probabilistic Engineering Mechanics 3 (4) (1988) 207 – 217. doi:10.1016/0266-8920(88)90013-6.

[32] M. Misraji, M. Valdebenito, H. Jensen, C. Mayorga, Application of directional importance sampling for estimation of first excursion probabilities of linear structural systems subject to stochastic Gaussian loading, Mechanical Systems and Signal Processing 139 (2020) 106621. doi:10.1016/j.ymssp.2020.106621.

[33] G. Deodatis, Non-stationary stochastic vector processes: seismic ground motion applications, Probabilistic Engineering Mechanics 11 (3) (1996) 149 – 167. doi:10.1016/0266-8920(96)00007-0.

[34] A. Zerva, Spatial Variation of Seismic Ground Motions – Modeling and Engineering Applications, CRC Press, 2009.

[35] M. Shinozuka, Y. Sato, Simulation of nonstationary random process, Journal of the Engineering Mechanics Division 93 (1) (1967) 11–40.

[36] P. Weber, M. Fina, W. Wagner, Time domain simulation of earthquake excited buildings using a fuzzy stochastic approach, in: M. Beer, E. Zio (Eds.), Proceedings of the 29th European Safety and Reliability Conference (ESREL), Hannover, 2019, pp. 2243–2250.

[37] W. McGuire, R. Gallagher, R. Ziemian, Matrix structural analysis, John Wiley & Sons, 2000.

[38] A. Chopra, Dynamics of structures: theory and applications to earthquake engineering, Prentice Hall, 1995.

[39] W. Gautschi, Numerical Analysis, 2nd Edition, Birkhäuser Boston, 2012. doi:10.1007/978-0-8176-8259-0.

[40] H. Jensen, A. Sepulveda, Optimal design of uncertain systems under stochastic excitation, AIAA Journal 38 (11) (2000) 2133–2141.